Semiconductor Science and Technology

PAPER

Investigation of a minority carrier trap in a NiO/*β*-Ga_2O_3 *p*–*n* heterojunction via deep-level transient spectroscopy

To cite this article: Haolan Qu *et al* 2023 *Semicond. Sci. Technol.* **38** 105010

View the article online for updates and enhancements.

You may also like

- A state-of-art review on gallium oxide field-effect transistors
Rundi Qiao, Hongpeng Zhang, Shuting Zhao et al.

- Experimental investigation on the instability for NiO/-Ga_2O_3 heterojunction-gate FETs under negative bias stress
Zhuolin Jiang, Xiangnan Li, Xuanze Zhou et al.

- -Ga_2O_3 for wide-bandgap electronics and optoelectronics
Zbigniew Galazka

This content was downloaded from IP address 119.78.254.3 on 17/10/2023 at 09:54

IOP Publishing

Semiconductor Science and Technology

Semicond. Sci. Technol. **38** (2023) 105010 (7pp)

https://doi.org/10.1088/1361-6641/acf608

Investigation of a minority carrier trap in a NiO/β-Ga_2O_3 *p–n* heterojunction via deep-level transient spectroscopy

Haolan Qu[1,2,3], Jiaxiang Chen[1,2,3], Yu Zhang[1,2,3], Jin Sui[1,2,3], Ruohan Zhang[1,4], Junmin Zhou[1,2,3], Xing Lu[5] and Xinbo Zou[1,4,*]

[1] School of Information Science and Technology, ShanghaiTech University, Shanghai 201210, People's Republic of China
[2] Shanghai Institute of Microsystem and Information Technology, Chinese Academy of Sciences, Shanghai 200050, People's Republic of China
[3] School of Microelectronics, University of Chinese Academy of Sciences, Beijing 100049, People's Republic of China
[4] Shanghai Engineering Research Center of Energy Efficient and Custom AI IC, Shanghai 200031, People's Republic of China
[5] School of Electronics and Information Technology, Sun Yat-sen University, Guangzhou 510275, People's Republic of China

E-mail: zouxb@shanghaitech.edu.cn

Received 24 April 2023, revised 26 July 2023
Accepted for publication 1 September 2023
Published 11 September 2023

Abstract

The properties of a minority carrier (hole) trap in β-Ga_2O_3 have been explicitly investigated using a NiO/β-Ga_2O_3 *p–n* heterojunction. Via deep-level transient spectroscopy, the activation energy for emission (E_{emi}) and the hole capture cross section (σ_p) were derived to be 0.10 eV and 2.48 $\times$ 10^{-15} cm^2, respectively. Temperature-enhanced capture and emission kinetics were revealed by the decrease in the capture time constant (τ_c) and emission time constant (τ_e). Moreover, it was determined that the emission process of the minority carrier trap is independent of the electric field. Taking carrier recombination into account, a corrected trap concentration (N_{Ta}) of 2.73 $\times$ 10^{15} cm^{-3} was extracted, together with an electron capture cross section (σ_n) of 1.42 $\times$ 10^{-18} cm^2. This study provides a foundation for the comprehension of trap properties in β-Ga_2O_3, which is crucial for overcoming self-trapped hole effects when obtaining *p*-type β-Ga_2O_3 materials and performance enhancement of β-Ga_2O_3-based power devices.

Keywords: NiO/β-Ga_2O_3*p–n* heterojunction, deep-level transient spectroscopy, minority carrier trap, time constant, trap concentration

(Some figures may appear in colour only in the online journal)

1. Introduction

Today, β-Ga_2O_3 has tremendous potential in power supply, radar and communication systems due to its outstanding material properties, including its wide bandgap (4.9 eV), high breakdown electric field (8 MV cm^{-1}) and availability of single-crystal native substrates [1, 2]. In the past, in addition to unipolar devices [3–5], enormous efforts have been made in the development of β-Ga_2O_3-based bipolar devices [6–9]. However, *p*-type β-Ga_2O_3 represents a challenge due to its large hole effective mass and self-trapping of holes in β-Ga_2O_3 [2, 10]. Instead, β-Ga_2O_3-based *p–n* heterojunctions have typically been manufactured with other *p*-type materials, such as Si [11], GaN [12, 13], NiO [6, 8, 14], 4H-SiC [7], diamond [15], $CuMo_2$ [16] and $ZnCo_2O_4$ [8]. For instance,

* Author to whom any correspondence should be addressed.

© 2023 IOP Publishing Ltd

the NiO/β-Ga_2O_3 *p*–*n* heterojunction has successfully demonstrated a low specific on resistance of 2.7 mΩ cm^2 and a high breakdown voltage of 1404 V [6].

It is also reported that the performance of the β-Ga_2O_3 *p*–*n* heterojunction is significantly affected by deep-level traps inside the devices [17–19]. By reducing the deep-level trap concentration, improved performance was obtained in the NiO/β-Ga_2O_3 *p*–*n* heterojunction, including a reduced ideality factor and an enlarged reverse blocking voltage [17]. Furthermore, a previous study suggested that the forward conduction characteristics of the NiO/β-Ga_2O_3 *p*–*n* heterojunction were primarily governed by Shockley–Read–Hall recombination induced by interfacial states or mid-gap traps [18].

There have been some investigations on the majority carrier (electron) traps in the β-Ga_2O_3 *p*–*n* heterojunction [8, 13, 15, 17–20]. In a NiO/β-Ga_2O_3 *p*–*n* heterojunction, two majority carrier traps were identified and believed to be responsible for the forward subthreshold conduction ($E_C - 0.67$ eV) and reverse leakage current at a high electric field ($E_C - 0.75$ eV), respectively [19].

Compared to majority carrier traps, there are few studies on minority carrier (hole) traps in *n*-type β-Ga_2O_3. A minority carrier trap with an activation energy for emission (E_{emi}) of 0.14 eV was found in a NiO/β-Ga_2O_3 *p*–*n* heterojunction [18, 19] and a diamond/β-Ga_2O_3 *p*–*n* heterojunction [15]. However, some issues still need to be addressed before one can achieve complete comprehension of minority carrier traps in β-Ga_2O_3 *p*–*n* heterojunctions.

(a) Few studies focus on the capture process characteristics of minority carrier traps in β-Ga_2O_3, such as the temperature-dependent capture time constant (τ_c) and the capture barrier energy (E_{cap}). The lack of the above information may hinder crucial optimization of β-Ga_2O_3-based bipolar devices. For example, the capture process of minority carrier traps in a high-gain β-Ga_2O_3 ultraviolet detector is highly related to the gain and spectral responsivities of the photodetector [21].
(b) Information on the emission process of minority carrier traps is critical in understanding the correlation between minority carrier traps and device properties, such as compensation of conductivity and recombination of nonequilibrium charge carriers [22]. The electric-field-dependent emission process has previously been qualitatively investigated [18]; however, a quantitative assessment of the emission time constant (τ_e) of minority carrier traps in β-Ga_2O_3 *p*–*n* heterojunctions is still missing.
(c) The minority carrier trap concentration has previously been extracted using deep-level transient spectroscopy (DLTS) [18, 19]. Nevertheless, failure to take the quick carrier recombination effect into account would lead to an underestimated trap concentration rather than the actual value. It is highly demanding to accurately extract the trap concentration (N_T), which is key to identifying the origins of traps and providing feedback for the optimization of materials and devices [23].

In this paper, the electrical and trap characteristics of a NiO/β-Ga_2O_3 *p*–*n* heterojunction were thoroughly studied. A minority carrier (hole) trap ($E_V + 0.10$ eV) is extracted via DLTS in a NiO/β-Ga_2O_3 *p*–*n* heterojunction. The temperature-dependent τ_c is determined by varying the filling pulse width (t_P), from which the E_{cap} is measured. The negligible shift of τ_e with an altering reverse bias (U_R) indicates an electric-field-independent emission process. Meanwhile, temperature-enhanced emission behavior is revealed by the temperature-dependent τ_e. By varying the U_R, a corrected trap concentration (N_{Ta}) is obtained together with the electron capture cross section (σ_n). The investigation on the minority carrier trap paves a solid path for a comprehensive understanding of the trap properties in β-Ga_2O_3 *p*–*n* heterojunctions, which could further facilitate acquisition of *p*-type β-Ga_2O_3 and performance enhancement of β-Ga_2O_3-based devices.

2. Device and electrical characteristics

Figure 1(a) shows a schematic cross section of the NiO/β-Ga_2O_3 *p*–*n* heterojunction. The wafer contained a 10 μm thick Si-doped n^--type β-Ga_2O_3 drift layer and a 635 μm thick Sn-doped (001) n^+-type β-Ga_2O_3 substrate, and their electron concentrations were about 4×10^{16} cm^{-3} and 9.7×10^{18} cm^{-3}, respectively. A Ti/Au (20 nm/80 nm) cathode was formed by electron beam evaporation and rapid thermal annealing for 60 s at 470 °C. Subsequently, the 360 nm thick SiO_2 and 40 nm thick SiN_x were grown by plasma-enhanced chemical vapor deposition. To pattern the *p*-type NiO region, inductively coupled plasma etching was applied for 160 s, followed by buffered oxide etchant treatment for 30 s to remove residual SiO_2. Then, 300 nm thick *p*-type NiO with a radius of 110 μm was deposited by sputtering and lift-off. The hole concentration in the *p*-type NiO layer is 3.7×10^{19} cm^{-3} via Hall measurements. Eventually, a circular Ni/Au (50 nm/100 nm) anode with a radius of 100 μm was formed after metal deposition and annealing at 300 °C for 120 s.

Figure 1(b) illustrates the forward and reverse current–voltage (*I*–*V*) characteristics of the NiO/β-Ga_2O_3 *p*–*n* heterojunction at 300 K. A leakage current of 7.09×10^{-9} A cm^{-2} at a bias of -50 V is observed, deducing an excellent voltage-blocking capacity. The forward *I*–*V* characteristics in linear scale are plotted in the inset of figure 1(b), and the threshold voltage (V_{th}) is determined to be 1.84 V at 300 K, using 1 A cm^{-2} standard.

Figure 1(c) displays the capacitance–voltage (*C*–*V*) characteristics of the NiO/β-Ga_2O_3 *p*–*n* heterojunction at 1 MHz with a step of 50 K. To investigate the relationship between capacitance and temperature, the capacitance–temperature (*C*–*T*) characteristics at -0.75 V are exhibited in figure 1(d). The capacitance reduces from 23.50 nF cm^{-2} to 13.80 nF cm^{-2} as the temperature decreases from 350 K to 25 K due to the reduced hole concentration in *p*-type NiO

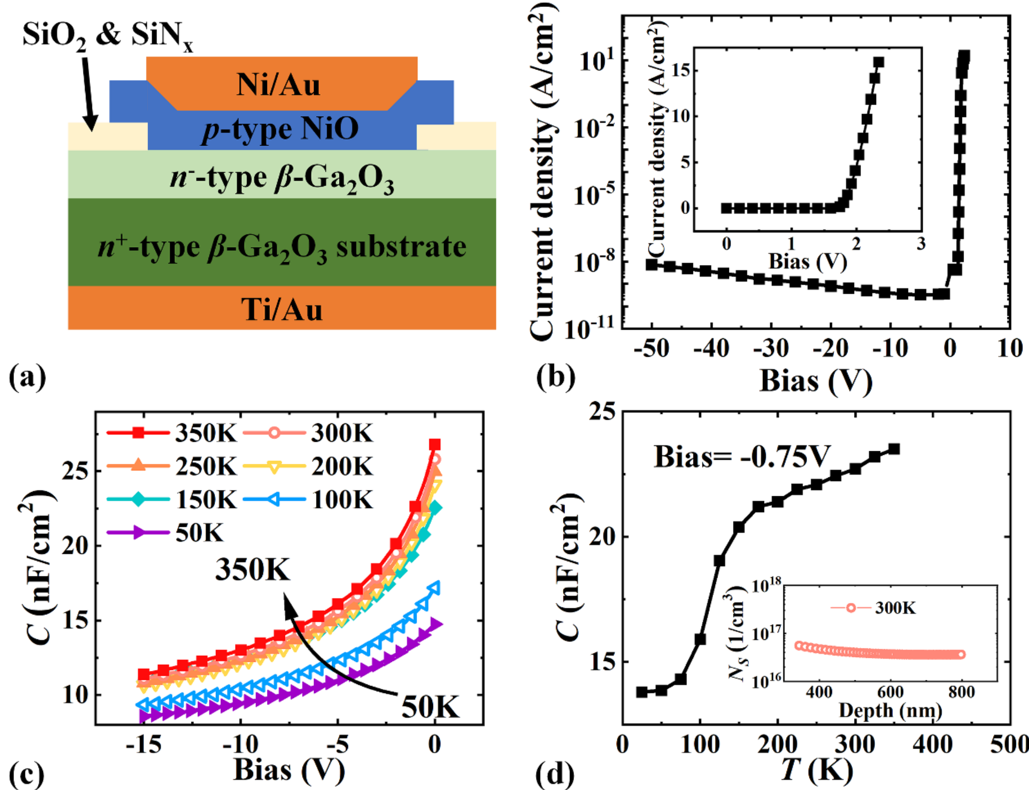

Figure 1. (a) A schematic cross section of the NiO/β-Ga_2O_3 p–n heterojunction. (b) Forward and reverse I–V characteristics on a logarithmic scale at 300 K. Inset: forward I–V characteristics in linear scale at 300 K. (c) C–V characteristics from 50 K to 350 K. (d) C–T characteristics. Inset: the carrier concentration extracted from the C–V characteristics at 300 K.

at low temperatures [18]. Moreover, the capacitance was extracted to be 13.80 nF cm^{-2} at 25 K, indicating that the hole concentration was nearly halved at cryogenic temperatures. Meanwhile, the depletion region in the junction mainly locates at the n^--type β-Ga_2O_3 layer, as the hole concentration in the p-type NiO layer is still much larger than the carrier concentration in the n^--type β-Ga_2O_3 layer, even though about half of the holes are frozen out at low temperatures. As shown in the inset of figure 1(d), the carrier concentration (N_S) was extracted to be about 4 × 10^{16} cm^{-3} at 300 K.

3. Trap characteristics

As depicted in figure 2(a), the trap properties have been quantified by temperature-scanning DLTS from 20 K to 350 K. The equipment used in this experiment is the FT 1230 high-energy resolution analysis DLTS (FT 1230 HERA-DLTS) system (PhysTech). The DLTS signal is recorded with a reverse bias $U_R = -15$ V, a filling pulse $U_P = -0.1$ V, a filling pulse width $t_P = 0.01$ s and a measurement period $T_W = 0.01$ s. A minority carrier trap (H1) was determined by a distinct negative valley in the DLTS spectrum. When the pulse bias changes from −15 V to −0.1 V, the junction barrier between NiO and β-Ga_2O_3 becomes smaller, and it is easier for holes to get injected from p-type NiO into n^--type β-Ga_2O_3 directly or via the assistance of an interface state. As shown in figure 2(b), H1 features an E_{emi} of 0.10 eV and a hole capture cross section (σ_p) of 2.48 × 10^{-15} cm^2 by Arrhenius analysis [24]. Furthermore, the depletion region width with U_R of −15 V is evaluated to be 1.24 μm around 60 K, which is much smaller than the thickness of n^--type β-Ga_2O_3 (10 μm), deducing that H1 is located in the upper region of n^--type β-Ga_2O_3.

As shown in table 1, hole traps or defects in β-Ga_2O_3 have been commonly observed in the literature [18, 19]. Hole traps with comparable E_{emi} and smaller σ_p were reported in both the Si-doped β-Ga_2O_3 drift layer ($E_{emi} = 0.14$ eV, σ_p = 6–7 × 10^{-17} cm^2) and the unintentionally doped β-Ga_2O_3 bulk substrate ($E_{emi} = 0.06$ eV, σ_p = 1–2 × 10^{-21} cm^2) [18, 19]. Compared to other hole traps, the larger σ_p of H1 indicates the enhanced ability of H1 to capture holes in β-Ga_2O_3. The strong capability of H1 to capture holes represents the barrier which needs to be overcome before achieving p-type conduction in β-Ga_2O_3 materials.

The variations of capacitance transient amplitudes ($\triangle C$) with different t_P were recorded from 40 K to 60 K, as shown in figure 3(a). As t_P increases, the absolute value of $\triangle C$ exhibits a steep increase initially due to the incremental amount of filled trap. However, the value of $\triangle C$ becomes saturated while t_P is further enhanced, which is attributed to the complete

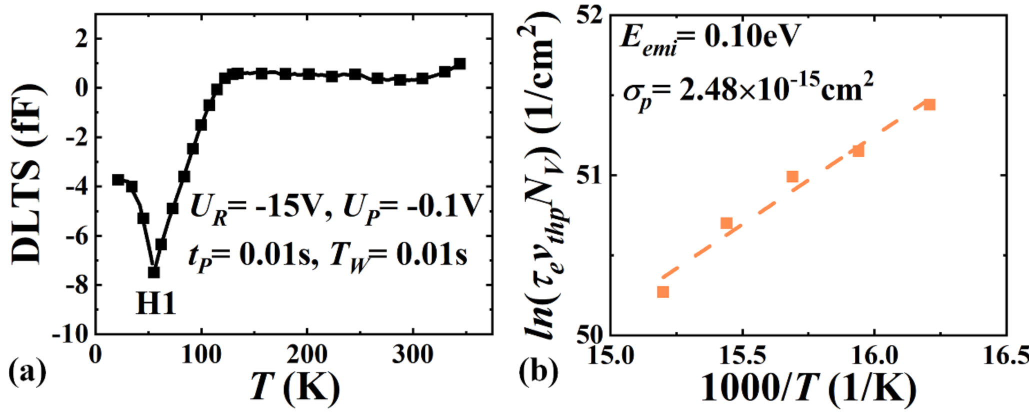

Figure 2. (a) The temperature-scanning DLTS signal at 1 MHz. (b) The Arrhenius plot of H1 to extract E_{emi}, where v_{thp} is the thermal velocity of holes and N_V is the effective density of states in the conduction band.

Table 1. A comparison of trap properties between H1 and other hole traps in the literature. (NA means not applicable in the table.)

E_{emi} (eV)	β-Ga_2O_3 structure	σ_p (cm^2)
0.10 [This work]	Si-doped epilayer	2.48×10^{-15}
0.14 [18]	Si-doped epilayer	$6–7 \times 10^{-17}$
0.06 [19]	Unintentionally doped bulk material	$1–2 \times 10^{-21}$

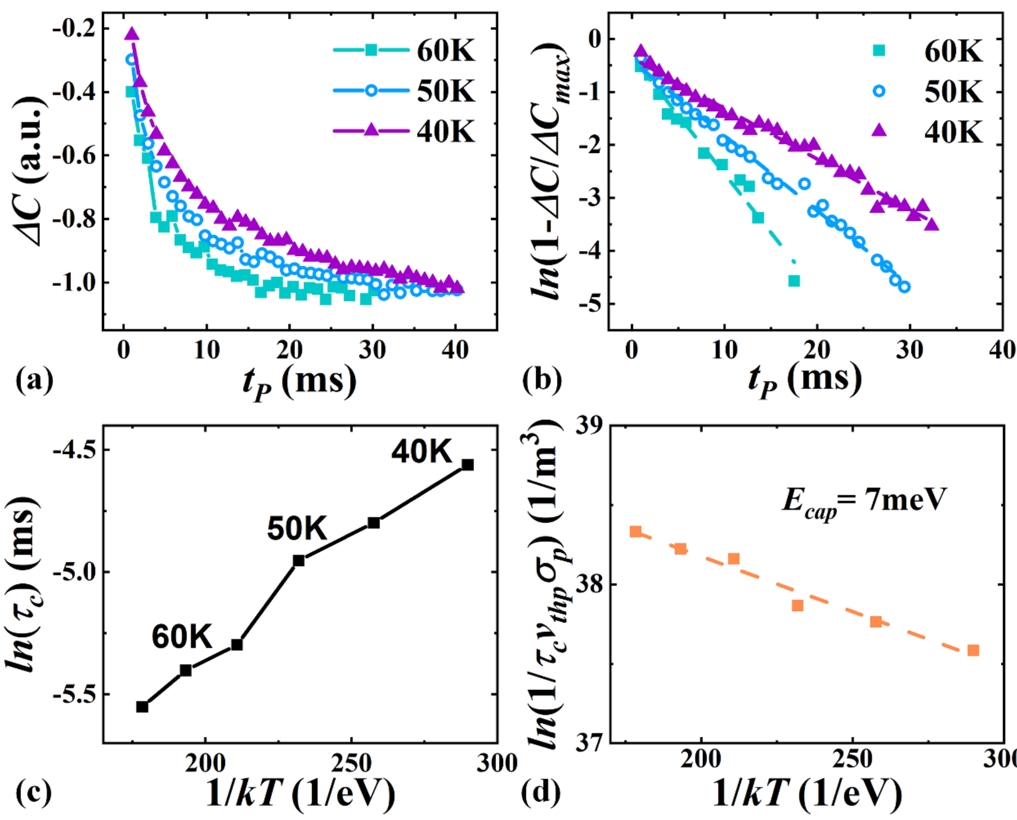

Figure 3. (a) The normalized $\triangle C$ as a function of t_P. (b) Fitting curves for H1. (c) The capture time constant from 40 K to 65 K. (d) An Arrhenius plot of H1 to extract E_{cap}.

occupancy of traps. When the temperature rises, a shorter t_P is sufficient to achieve the saturation of $\triangle C$, indicating that the capture process of H1 is accelerated at a higher temperature.

Figure 3(b) illustrates the relationship between $\triangle C$ and t_P at different temperatures, showing good linearity, as described by the following equation [25]:

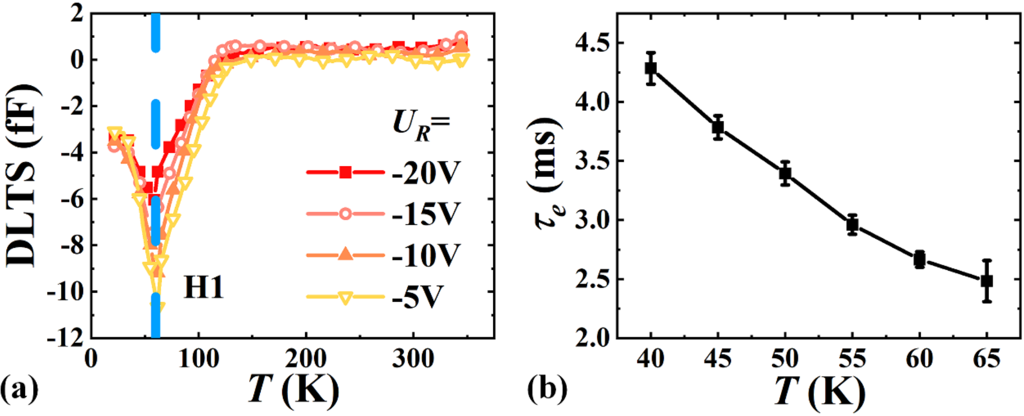

Figure 4. (a) The temperature-scanning DLTS signal with different U_R. (b) The temperature-dependent τ_e.

$$\ln\left(1-\frac{\Delta C}{\Delta C_{\max}}\right)=\frac{t_P}{\tau_c} \quad (1)$$

where $\triangle C_{\max}$ is the saturated capacitance transient amplitude. H1 is regarded as a point defect rather than an extended defect as a result of the excellent fitting linearity [25]. In figure 3(c), from 40 K to 65 K, τ_c obtained via equation (1) reduces from 10.45 ms to 3.88 ms, revealing a temperature-enhanced capture process. It is also proposed that τ_c has the following relationship with temperature, from which E_{cap} can be determined [26]:

$$\ln\left(\frac{1}{\tau_c v_{\mathrm{thp}}\sigma_p}\right)=-\frac{E_{\mathrm{cap}}}{kT}+\ln\left(p_P\right) \quad (2)$$

where k is the Boltzmann constant, and p_P is the hole concentration at the depletion region width with U_P (w_P). As shown in figures 3(d) and (a), a negligible E_{cap} (7 meV) is extracted by linear fitting of equation (2). Due to the absence of a capture barrier for H1, holes in β-Ga_2O_3 are readily captured by H1, posing a significant obstacle in the manufacture of p-type β-Ga_2O_3 materials.

The binding energy (E_{binding}), which signifies the distance between the trap and valence band, is extracted to be 0.10 eV from the following equation [27]:

$$E_{\mathrm{emi}}=E_{\mathrm{cap}}+E_{\mathrm{binding}} \quad . \quad (3)$$

Due to the absence of E_{cap}, E_{binding}, which represents the precise location of H1 in the bandgap, is typically equal to E_{emi}.

Figure 4(a) depicts the temperature-scanning DLTS signal with different U_R. The blue dashed line represents the valley of the temperature-scanning DLTS signal. The valley position stabilizes at around 60 K as U_R increases, indicating that H1 is a bulk trap in n^--type β-Ga_2O_3 instead of an interface trap [28]. Meanwhile, the fixed valley position also infers that the emission process is not enhanced by the rising electric field, corresponding to U_R from -5 V to -20 V [28]. Figure 4(b) shows the τ_e extracted by isothermal DLTS, as enhancing the reverse bias from -5 V to -20 V, in the temperature ranging from 40 K to 65 K [3]. The bar in the graph represents the deviation value of $\tau_{e,}$ as varying U_R. When U_R increases, τ_e is slightly shifted, leading to a typical electric-field-independent emission process. Nonetheless, the decrease in τ_e from 4.28 ms to 2.48 ms when the temperature increases from 40 K to 65 K reveals a temperature-enhanced emission process.

Figure 5(a) shows the N_T derived from $\triangle C$ as a function of the depletion region width under the U_R (w_R) by isothermal DLTS with varying U_R:

$$N_T=2\frac{\Delta C}{C_R}N_S \quad (4)$$

where C_R is the capacitance at U_R. During isothermal DLTS, t_P is set to be 100 ms to ensure that all the traps are occupied. The N_T initially increases and subsequently decreases as w_R is extended. The increase in the N_T is related to the quick carrier recombination effect at the edge of the depletion region [29]. The electron concentration near the edge of the depletion region gradually drops to zero in the region with a critical width (λ_R), as shown in figure 5(b). In this region, holes are emitted rapidly from traps to recombine with the electrons, and fail to be detected by DLTS due to the short emission time. The neglection of quick carrier recombination contributes to an underestimated N_T. The N_{Ta}, which means the corrected trap concentration, can be extracted from the following equations [29]:

$$N_T=N_{\mathrm{Ta}}\left(1-\frac{\lambda_R}{w_R}\right)^2 \quad (5)$$

$$\lambda_R=\sqrt{\frac{2\varepsilon_r\varepsilon_0 kT}{N_S q^2}\ln\left(\frac{N_S v_{\mathrm{thn}}\sigma_n\tau_e}{\ln(2)}\right)} \quad (6)$$

where ε_r and ε_0 are relative and vacuum permittivity, separately, q is the elementary charge, and v_{thn} is the thermal velocity of electrons. From the fitting red dashed line, an N_{Ta} of 2.73×10^{15} cm^{-3}, a λ_R of 533 nm and a σ_n of 1.42×10^{-18} cm^2 are extracted. The N_{Ta} is one order of magnitude greater than the N_T, reflecting a higher consumption of

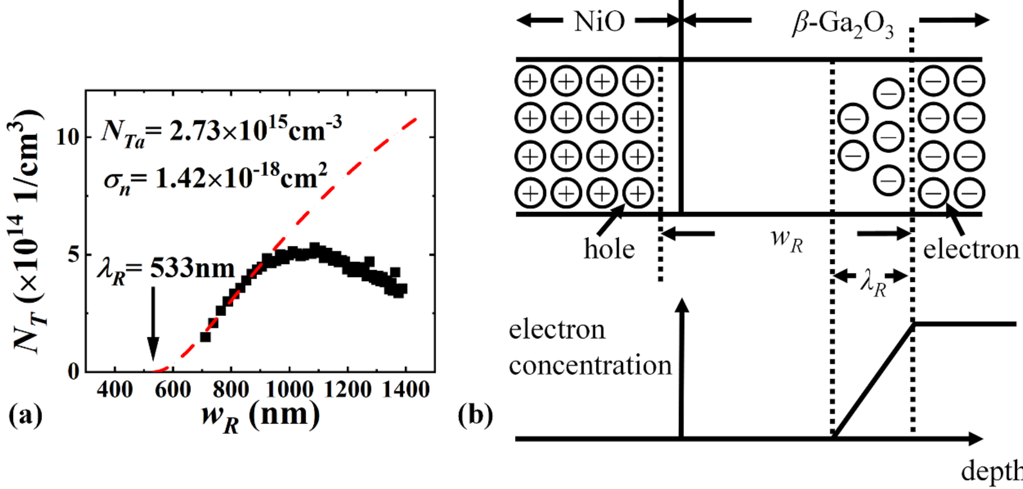

Figure 5. (a) N_T as a function of w_R. The red dashed line represents the fitting of equation (5). (b) The carrier distribution near the NiO/β-Ga_2O_3 interface.

holes than the result that does not take quick carrier recombination into account. Meanwhile, σ_n is much smaller than σ_p, suggesting that H1 is more likely to capture holes rather than electrons. The results highlight the difficulties associated with achieving efficient hole doping in β-Ga_2O_3. As w_R is further extended, N_T shows a decreasing trend, as shown in figure 5(a). The decreased N_T as extracted was due to insufficient hole injection. When w_R is adequately long, it is challenging for the holes to tunnel from *p*-type NiO and diffuse to the region far away from the NiO/β-Ga_2O_3 junction interface, and hole traps located far away from the NiO/β-Ga_2O_3 junction interface cannot be detected due to the absence of hole trapping activity.

4. Conclusion

In summary, the electrical and trap characteristics of a NiO/β-Ga_2O_3 *p*–*n* heterojunction were thoroughly investigated. A minority carrier trap H1 was identified via DLTS with an E_{emi} of 0.10 eV and σ_p of 2.48 × 10^{-15} cm^2, and is regarded as a point defect. When the temperature elevates from 40 K to 65 K, τ_c drops from 10.45 ms to 3.88 ms and τ_e decreases from 4.28 ms to 2.48 ms, indicating a temperature-enhanced capture and emission process. In contrast, τ_e remains unchanged with varying U_R, inferring the insignificant influence of the electric field on the emission process. Taking the quick carrier recombination effect into account, N_{Ta} and σ_n were measured to be 2.73 × 10^{15} cm^{-3} and 1.42 × 10^{-18} cm^2, respectively. The results imply that the strong capability of capturing holes, a large corrected trap concentration and the absence of a capture barrier, in combination, represent obstacles that need to be overcome before achieving good *p*-type conduction in β-Ga_2O_3 materials. The trap properties revealed in this study also provide a foundation for understanding trap-related dynamic degradation in β-Ga_2O_3-based power devices.

Data availability statement

All data that support the findings of this study are included within the article (and any supplementary files).

Acknowledgments

This work was supported by ShanghaiTech University Startup Fund 2017F0203-000-14, the National Natural Science Foundation of China (Grant No. 52131303), the Natural Science Foundation of Shanghai (Grant No. 22ZR1442300), and in part by CAS Strategic Science and Technology Program under Grant No. XDA18000000.

ORCID iDs

Haolan Qu https://orcid.org/0000-0002-2907-6565
Jiaxiang Chen https://orcid.org/0000-0001-6793-4025
Yu Zhang https://orcid.org/0000-0002-5017-6771
Jin Sui https://orcid.org/0000-0001-8884-8097
Junmin Zhou https://orcid.org/0009-0001-4630-9869
Xing Lu https://orcid.org/0000-0001-5808-9552
Xinbo Zou https://orcid.org/0000-0002-9031-8519

References

[1] Chabak K D *et al* 2019 *Semicond. Sci. Technol.* **35** 013002
[2] Pearton S, Ren F, Tadjer M and Kim J 2018 *J. Appl. Phys.* **124** 220901
[3] Qu H, Chen J, Zhang Y, Sui J, Gu Y, Deng Y, Su D, Zhang R, Lu X and Zou X 2023 *Semicond. Sci. Technol.* **38** 015001
[4] Wong M H, Takeyama A, Makino T, Ohshima T, Sasaki K, Kuramata A, Yamakoshi S and Higashiwaki M 2018 *Appl. Phys. Lett.* **112** 023503
[5] Chen J, Luo H, Qu H, Zhu M, Guo H, Chen B, Lv Y, Lu X and Zou X 2021 *Semicond. Sci. Technol.* **36** 055015

[6] Luo H, Zhou X, Chen Z, Pei Y, Lu X and Wang G 2021 *IEEE Trans. Electron Devices* **68** 3991–6
[7] Yu J, Dong L, Peng B, Yuan L, Huang Y, Zhang L, Zhang Y and Jia R 2020 *J. Alloys Compd.* **821** 153532
[8] Schlupp P, Splith D, von Wenckstern H and Grundmann M 2019 *Phys. Status Solidi* a **216** 1800729
[9] Jia M, Wang F, Tang L, Xiang J, Teng K S and Lau S P 2020 *Nanoscale Res. Lett.* **15** 47
[10] Higashiwaki M, Sasaki K, Murakami H, Kumagai Y, Koukitu A, Kuramata A, Masui T and Yamakoshi S 2016 *Semicond. Sci. Technol.* **31** 034001
[11] Shin G, Kim H Y and Kim J 2018 *Korean J. Chem. Eng.* **35** 574–8
[12] Feng Q *et al* 2020 *ECS J. Solid State Sci. Technol.* **9** 035001
[13] Guo D *et al* 2018 *ACS Nano* **12** 12827–35
[14] Gong H, Chen X, Xu Y, Chen Y, Ren F, Liu B, Gu S, Zhang R and Ye J 2020 *IEEE Trans. Electron Devices* **67** 3341–7
[15] Polyakov A Y *et al* 2021 *J. Appl. Phys.* **129** 185701
[16] Wu C *et al* 2021 *Mater. Today Phys.* **17** 100335
[17] Gong H *et al* 2021 *IEEE J. Electron Devices Soc.* **9** 1166–71
[18] Wang Z *et al* 2022 *IEEE Trans. Electron Devices* **69** 981–7
[19] Wang Z, Gong H H, Yu X X, Ji X, Ren F F, Yang Y, Gu S, Zheng Y, Zhang R and Ye J 2023 *Sci. China Mater.* **66** 1157–64
[20] Wang Z P, Gong H H, Yu X X, Hu T C, Ji X L, Ren F F, Gu S L, Zheng Y D, Zhang R and Ye J D 2023 *Appl. Phys. Lett.* **122** 152102
[21] Li K H, Alfaraj N, Kang C H, Braic L, Hedhili M N, Guo Z, Ng T K and Ooi B S 2019 *ACS Appl. Mater. Interfaces* **11** 35095–104
[22] Polyakov A Y, Lee I H, Smirnov N B, Shchemerov I V, Vasilev A A, Chernykh A V and Pearton S J 2020 *J. Phys. D: Appl. Phys.* **53** 304001
[23] Kanegae K, Narita T, Tomita K, Kachi T, Horita M, Kimoto T and Suda J 2020 *Jpn. J. Appl. Phys.* **59** SGGD05
[24] Lang D V 1974 *J. Appl. Phys.* **45** 3023–32
[25] Heo S *et al* 2016 *Sci. Rep.* **6** 30554
[26] Criado J, Gomez A, Calleja E and Muñoz E 1988 *Appl. Phys. Lett.* **52** 660–1
[27] Hacke P, Detchprohm T, Hiramatsu K, Sawaki N, Tadatomo K and Miyake K 1994 *J. Appl. Phys.* **76** 304–9
[28] Coelho A, Adam M and Boudinov H 2011 *J. Phys. D: Appl. Phys.* **44** 305303
[29] Kanegae K, Horita M, Kimoto T and Suda J 2018 *Appl. Phys. Express* **11** 071002